Available on CMS information server

CMS NOTE -2009/006

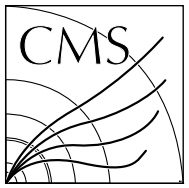

The Compact Muon Solenoid Experiment

CMS Note

Mailing address: CMS CERN, CH-1211 GENEVA 23, Switzerland

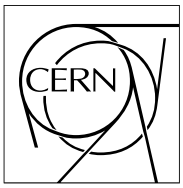

25 February 2009 (v4, 23 April 2009)

Mechanical Design and Material Budget of the CMS Barrel Pixel Detector

C. Amsler, K. Bösiger, V. Chiochia, R. Maier, Hp. Meyer, P. Robmann, S. Scherr, A. Schmidt, S. Steiner

Physik-Institut, Universität Zürich, Switzerland

W. Erdmann, K. Gabathuler, R. Horisberger, S. König, D. Kotlinski, B. Meier, S. Streuli

Paul Scherrer Institut, Villigen, Switzerland

A. Rizzi

Institute for Particle Physics, ETH Zürich, Switzerland

Abstract

The Compact Muon Solenoid experiment at the Large Hadron Collider at CERN includes a silicon pixel detector as its innermost component. Its main task is the precise reconstruction of charged particles close to the primary interaction vertex. This paper gives an overview of the mechanical requirements and design choices for the barrel pixel detector. The distribution of material in the detector as well as its description in the Monte Carlo simulation are discussed in detail.

1 Introduction

At the LHC design luminosity of $10^{34}\ \mathrm{cm}^{-2}\mathrm{s}^{-1}$, about 1000 particles will be traversing the tracker for each bunch crossing every $25\ \mathrm{ns}$. At a radius of $4\ \mathrm{cm}$ this corresponds to a hit rate density of $1\ \mathrm{MHz/mm}^2$. The tracker is required to operate in this high radiation environment with a reasonable lifetime of several years. The trajectories of charged particles need to be measured efficiently and with high precision. The amount of material needs to be kept to a minimum in order to limit effects such as multiple scattering, bremsstrahlung, photon conversions and nuclear interactions. These requirements and limitations strongly suggested an all-silicon design.

The CMS tracking detector consists of $200\ \mathrm{m}^2$ of active silicon. It is therefore the largest silicon tracking device ever built [1, 2, 3].

The pixel detector as the innermost part of CMS consists of three barrel layers at radii of 4.4, 7.4 and $10.2\ \mathrm{cm}$, respectively, with a length of $53\ \mathrm{cm}$. It is completed by two forward disks on each side, located along the beam axis at $z = \pm 34.5\ \mathrm{cm}$ and $z = \pm 46.5\ \mathrm{cm}$, extending in radius from $6\ \mathrm{cm}$ to $15\ \mathrm{cm}$. The pixel detector has 66 million pixels in total, of which 48 millions belong to the barrel.

Details on the mechanical design of the pixel barrel detector (PXB) are given in Section 2, while the material budget is discussed in Section 3. The description of the detector in the Monte Carlo simulation is outlined in Section 4.

2 Detector Design

For the purpose of the following discussion the detector is subdivided into three logical parts: the central barrel (containing the detector modules), the endflange and the supply tube.

The PXB system is constructed in two half-shells so that the insertion into the detector after the beam pipe installation is facilitated. A sketch of one half-shell is shown in Figure 1. The three half-barrel layers and the detector endflanges are clearly visible. The arrangement of the detector modules in ladders is indicated. The supply tube is not shown in this picture (see Figure 6 below).

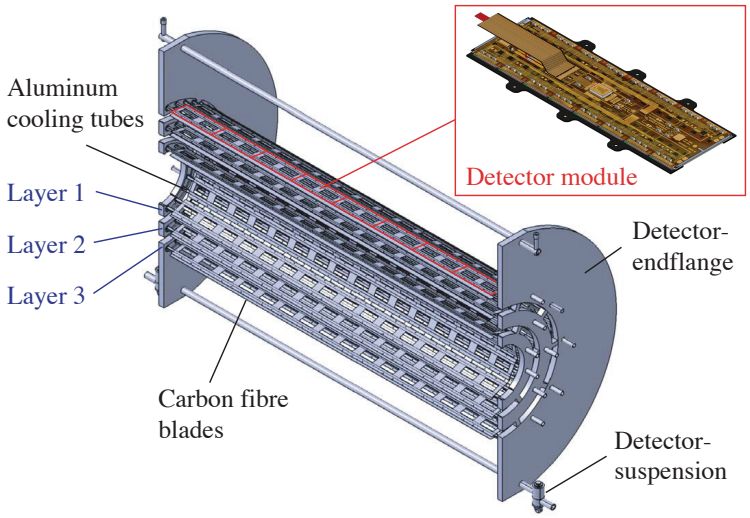

Figure 1: Sketch of one half of the pixel barrel detector including the endflanges.

2.1 Central Barrel

The skeleton of the central barrel is made of aluminum cooling pipes of trapezoidal shape with $0.3\ \mathrm{mm}$ wall thickness and $55.5\ \mathrm{cm}$ length. They are arranged in a way that thin carbon fiber ladders of $0.22\ \mathrm{mm}$ thickness can be glued on alternating sides as shown in Figure 2 [4]. The detector modules are then screwed to the carbon fiber ladders. The half-layers 1, 2 and 3 contain 8, 14 and 20 ladders, respectively. The number of cooling pipes is 9, 15 and 21, respectively. Each layer is completed by two half-modules (and half-ladders) at both edges (Figure 2).

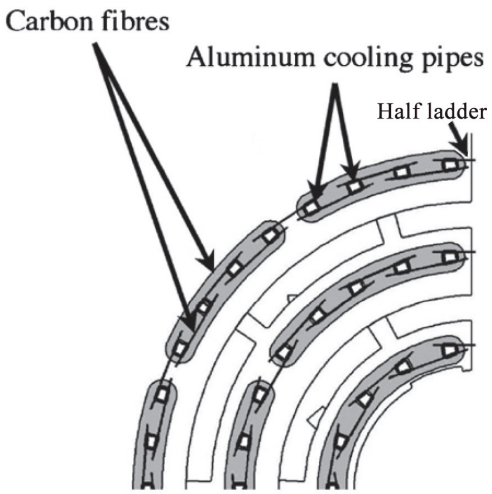

Figure 2: Sketch of the carbon fiber ladders mounted on aluminum cooling pipes.

Eight modules are mounted on each ladder. A module consists of the following components [5]:

- 250 μm thick silicon nitride basestrips supporting the modules,
- sensors made of 285 μm thick DOFZ-silicon [6],
- 8 or 16 Read-out Chips (ROCs) [7] with 52×80 pixels of size 150×100 $\mu\mathrm{m}^2$,
- a High Density Interconnect (HDI), a flexible low mass three-layer PCB (flex print),
- a Token Bit Manager (TBM) chip controlling the readout of the ROCs [8],
- signal and power cables.

A complete module has the dimensions 66.6×26.0 mm^2 and weighs 2.2 g plus up to 1.3 g for cables. More than half of the modules weight is due to the silicon (1.4 g) in the sensors and the ROCs. The temperature of the sensors will be maintained at $-10°$C. Details about the module and sensor design, performance and assembly can be found in Ref. [5, 9].

The signal and power cables run parallel to the modules along the z-direction. They are fed through the spacings in the endflange and are then radially distributed until they connect to the Printed Circuit Boards (PCBs) at the detector endflange.

The envelope of the central barrel region is defined by an internal and an external shielding at $r = 3.7$ cm and $r = 18.6$ cm extending over the full length of the barrel (57 cm). Both inner and outer shieldings are made of a 250 μm thick Kevlar® cylinder sandwiched between two 25 μm aluminum layers.

2.2 Endflange

The endflanges serve several purposes. They act as support structure for the whole barrel, distribute the coolant and hold electronic devices (endring prints) which are mounted circularly at the outer part of the endflanges.

An illustration of the layout is shown in Figure 3. Each half-disk contains 10 aluminum containers acting as manifolds to distribute the cooling fluid. Liquid fluorocarbon (C_6F_{14}) is used as coolant in the whole CMS tracker. The trapezoidal aluminum cooling pipes, described in Section 2.1, are laser welded to the containers with highest precision to guarantee leak tightness of the cooling system [10]. The side of the endflange facing the supply tube is equipped with "L" shaped cooling bends, one for each aluminum manifold, which facilitate the connection of flexible cooling lines (see Figure 5).

The half-disks are made of three arcs which are connected by 8 fittings as shown in Figure 3. The space between the arcs is used as feedthrough for the signal cables connecting the modules with the endflange electronics.

The dimensions of the endflange components are given in Table 1.

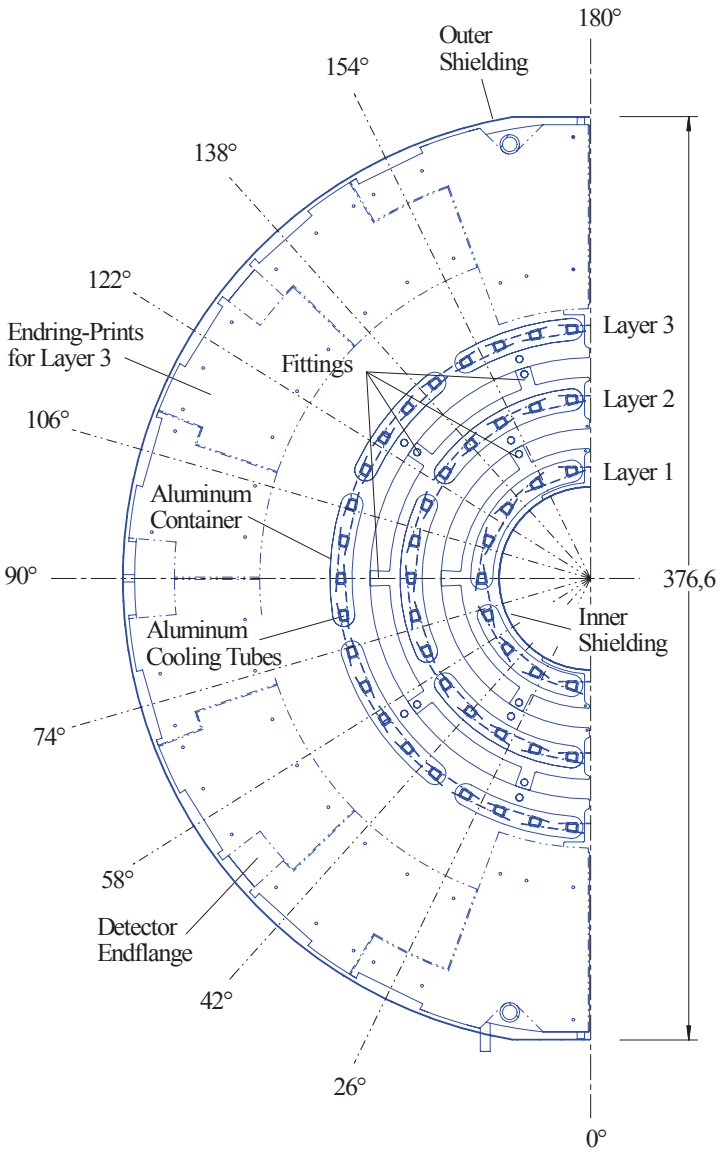

Figure 3: Drawing of the layout of the PXB endflange.

Table 1: Dimensions of the PXB endflanges in [cm].

	Layer 1	Layer 2	Layer 3
inner radius	3.75	6.1	9
outer radius	5.3	8.2	18.6
thickness	0.78		

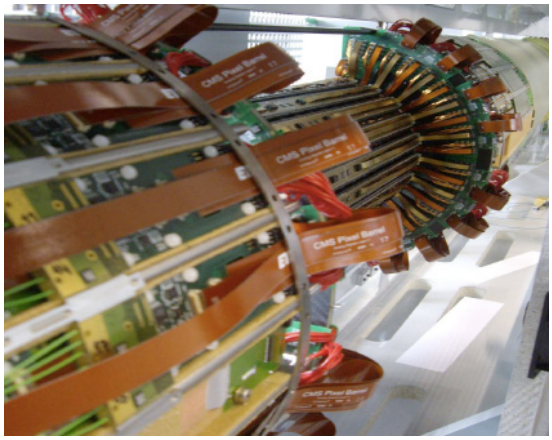

Figure 4: Photograph of the PXB detector. The supply tube is visible on the left half of the picture. The part in the middle shows the third layer of detector modules. The endflange with the radial cabling is visible on the upper right.

The endflange is made of a thin fiberglass frame filled with low density Airex® foam [11]. Both sides are covered with $0.5\ \mathrm{mm}$ thick carbon fiber plates, glued on either side. This technique provides the necessary stability and precision at a very low mass.

The layer 3 arc extends radially up to $18.6\ \mathrm{cm}$ and holds electronics equipment, the endring prints, which are fixed to the flange with custom made aluminum clamps. They act as interconnect between the modules and the supply tube electronics. The area between the radius $10.7\ \mathrm{cm}$ and $18.6\ \mathrm{cm}$ is almost fully covered by the endring PCBs on both sides of the endflange. They contain low current differential signal (LCDS) transceivers and cable connectors. More details about their functionality are available in [8].

As visible in Figure 4, the cables cover a large fraction of the endring prints and contribute a significant part to the total amount of metal in the vicinity of the endflange. This is discussed in more detail in Section 3.

All connections between the barrel detector and the supply tube run through the barrel endflange. The connections are flexible to a certain extent to allow small movements of the pixel detector. Also the cooling pipes connecting to the manifolds in the endflange are made of flexible material, silicone rubber reinforced with fiberglass. These cooling lines are distributed radially in the $r-\phi$ plane at $z = \pm 30.5\ \mathrm{cm}$ and are fixed with steel clamps to the "L" shaped cooling bends on the endflange and supply tube.

2.3 Supply Tube

The supply tube, one at each end of the pixel barrel, connects the PXB detector to the outside world. It contains the power cables, optical signal cables, and cooling lines. The tube is constructed in two half shells at both ends of the detector. Its position with respect to the barrel is shown in Figure 5. The tube has a length of $2.2\ \mathrm{m}$ and an inner radius of $18\ \mathrm{cm}$ with a wall thickness between $1\ \mathrm{cm}$ and $3\ \mathrm{cm}$, depending on the z-position. It is subdivided into three logical sectors (sectors A, B and C), as shown in Figure 6.

The supply tube also hosts several electronic devices, which are briefly described in the following: for the readout, the Analog Optical Hybrid (AOH) converts the analog signals to optical signals. The AOH includes the Analog Level Translator (ALT) chips. Six AOHs are placed in a single analog mother board.

For the detector control, digital signals are translated to optical signals in the Digital Optical Hybrid (DOH). The Phase Locked Loop (PLL) chips are used to split the clock from the trigger and the DELAY25 chips adjust the relative phases of all control signals. The Gate-Keeper chips convert the Low Voltage Differential Signals (LVDS) used by PLLs and DELAY25s to low current differential signals (LCDS) used by the pixel front-end chips. Two DOHs, 2 PLLs, 2 DELAY25s and 2 Gate-Keepers are placed on a single digital-motherboard.

The analog and digital mother boards are plugged into a single board called the opto-board.

To configure the AOHs and DOHs, the CCU chip (Communication and Control Unit) is used. For each half-shell of the supply tube a CCU-board, with 9 CCUs and 9 LVDS-MUX chips is used. More details can be found in [8].

The supporting elements of the structure are the stainless steel cooling tubes with a wall thickness of 0.1 mm run-

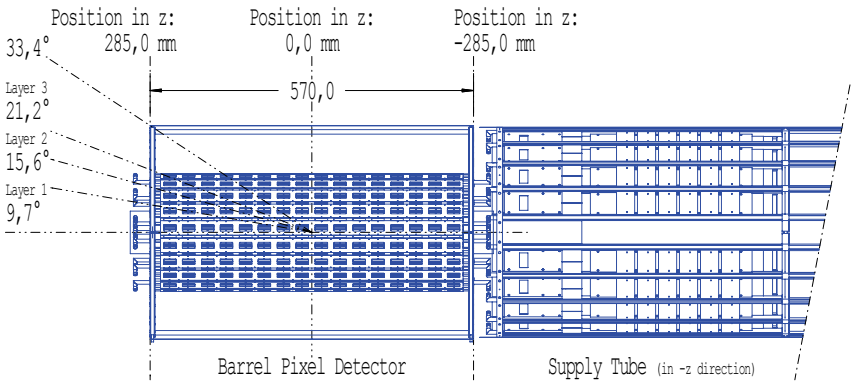

Figure 5: Pixel barrel detector (on the left) connecting to the supply tube (on the right). The ”L” shaped cooling bends are visible just outside the rectangle on the left edge, and between barrel and supply tube.

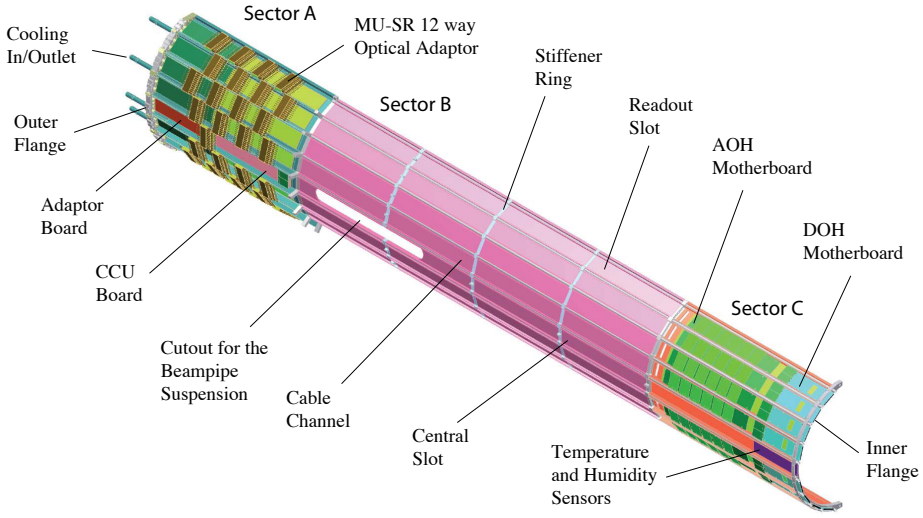

Figure 6: Illustration of the pixel barrel supply tube half-shell. It is subdivided into three logical sectors. Sector A is the leftmost part. The part in the middle (the four segments are visible) is Sector B. The innermost part (connecting to the endflange) is labelled Sector C.

ning along the z-direction. They are connected to the stiffener rings (fiberglass) and the inner and outer aluminum flanges. The gaps in-between are filled with foamed material (Airex®) to guarantee the required rigidity. All power and slow control lines are embedded in the supply tube body. This allows a clear layout of the wiring and makes the system also more reliable.

3 Material Budget

The amount of material given in the following tables was partially obtained by direct weight measurements of the components and partially calculated from design drawings. For instance, only the final total weight of the endflange support structure (without aluminum manifolds, electronics and coolant) could be determined by measurement due to the complexity of the construction process. Another example is the fraction of copper in the printed circuit boards which needed to be estimated based on the design drawings. Therefore the detailed composition of the various material fractions is subject to uncertainties in several cases. The calculated total weights of the substructures agree within a few percent with the real weights of the detector components. The obtained precision is therefore sufficient for an adequate description of the detector in the Monte Carlo simulation.

The following tables summarize the amount of material in all of the detector components, according to the order of discussion in the previous sections.

The material budget for the central barrel support structure is summarized in Table 2, which shows the total amount of aluminum, carbon fiber and coolant. The total material budget of the modules is given in Table 3.

Table 2: Material budget for the central barrel support structure (without modules and endflange) per half-shell in units of [g].

	Layer 1	Layer 2	Layer 3
carbon fiber	40	65	91
aluminum	52	86	120
coolant	75	126	176

Table 3: Total amount of material contained in the detector modules in [g] per detector half-shell. The sensors and ROCs are made of silicon. The module baseplates are made of silicon nitride and steel for screws and nuts. The materials Kapton®, copper, nickel, gold and solder belong to the HDI and its electrical components. Barium titanate is contained in the capacitors.

	Layer 1	Layer 2	Layer 3
silicon	100	166	232
silicon nitride	43	67	90
steel	7	12	17
glue	2.3	3.6	4.8
Kapton®	5.6	9.2	12.9
copper	4.1	6.8	9.6
nickel	0.9	1.4	2
gold	0.4	0.7	1
solder	4.8	7.7	10.6
barium titanate	12	19.7	27.4

Table 4: Material budget of signal and power cables in the central barrel region in [g] per detector half-shell.

	Layer 1	Layer 2	Layer 3
Kapton®	15	24	34
copper	12	19	27
aluminum	7	11	15

Since a ladder holds eight modules, there are four different cable lengths in the central barrel region: 23, 16, 9 and 3 cm. The power cables consist of an aluminum core with a copper and Kapton® coating, while the signal ribbon cables are made of 22 copper tracks and a Kapton® coating. Together, the cables have a mass occupancy of $0.034\ \mathrm{g/cm}$. Since the total cable length in the barrel is about $50\ \mathrm{m}$ per half-shell, they contribute to around $170\ \mathrm{g}$ to the material budget. The decomposition of the various materials for these cables is given in Table 4.

The inner shielding of the PXB detector weighs $65\ \mathrm{g}$ ($17\ \mathrm{g}$ aluminum and $48\ \mathrm{g}$ Kevlar®), while the outer shield weighs $320\ \mathrm{g}$ ($87\ \mathrm{g}$ aluminum and $233\ \mathrm{g}$ Kevlar®).

The endring PCBs mounted on the detector endflange (Table 5) consist of standard epoxy substrate in five layers of $68\ \mu\mathrm{m}$ thickness and two (four) copper layers of $18\ \mu\mathrm{m}$ ($25\ \mu\mathrm{m}$) thickness. Their material budget is given in the upper rows of Table 6.

As mentioned earlier, the signal cables connecting the modules with the endring electronics are running parallel to the beam axis above and below the modules until the cables reach the endflange (this material is given in Table 4). Depending on the longitudinal module position, a part of the cables is attributed to the central barrel region, while the remaining part belongs to the endflange. The length fractions on the endflange depend on the radial position of the corresponding connectors and the position of the feedthroughs. The material fraction which is attributed to the endflange is given in the middle part of Table 6.

A similar type of Kapton® cables, but with different width and length is used to connect the endring prints with the supply tube. In addition, power cables made of copper and aluminum, are connected at the edge of the endflange. These are summarized in the bottom part of Table 6.

The enflange and supply tube are also connected by cooling pipes. The pipes are made of silicone rubber ($46\ \mathrm{g}$ per half-disk) reinforced with fiberglass, containing $53\ \mathrm{g}$ of coolant.

The material decomposition for the three sectors of the supply tube is shown in Table 7.

4 Monte Carlo Simulation

In this section we describe the implementation of the material budget in the simulation software.

In the CMS software framework, the passage of particles through matter is simulated by the GEANT4 toolkit [12, 13]. Therefore, the exact position, amount and type of materials need to be specified. The access to the detector components and their geometry is provided by the Detector Description Database (DDD) [14]. The master data source for the DDD is a collection of files implemented in the Extensible Markup Language (XML) using the Detector Description Language. The detector is divided into logical volumes of one particular type of material. In many cases this is a mixture of the materials contained in the defined volume. For instance, screws are usually not represented as single volumes, but their material is mixed into the definition of a larger structure containing them.

The description in the Monte Carlo simulation needs to be as precise as possible in order to reproduce the exact amount of material interactions. Such interactions deteriorate the trajectories of particles and influence the measurements in the outer detectors (strip tracker, calorimeters and muon detectors). The sensitive volumes in the barrel have been described with the highest possible accuracy (Section 4.1). Also the endflanges are described with a high level of detail, since they are located directly in front of the sensitive volumes of the pixel forward detector. This is discussed in Section 4.2.

The supply tubes extend to the very forward region up to a pseudo-rapidity of $|\eta| = 3.4$, and are described in less detail in this region (Section 4.3).

In the following, the implementation of the detector geometry is outlined. The software representation is based on the material content discussed in the previous sections.

Table 5: Material decomposition of the PXB endflange in [g] per half-disk.

	Layer 1	Layer 2	Layer 3
carbon fiber	4	8.5	75
glass fiber	5.6	9	17
Airex®	0.4	1.3	21
aluminum	5.3	8.4	12
coolant	8	15.5	17.5
steel	5	7.5	12.5

Table 6: Material decomposition of the endring electronics including the cabling going to supply tube and modules in [g] per half-disk. The amount of solder is estimated. The term "plastics" refers to various types of polymers of similar density which are used in connectors and cable insulations.

	boards layer 1+2	boards layer 3
copper	32	27
FR4	26	22
plastics	33	15
solder	2.6	2.2
	cables to modules	
	signal cables	power cables
copper	12.1	9.2
Kapton®	26	1.25
aluminum	-	11.7
	cables to supply tube	
	power cables	signal cables
copper	29	24
Kapton®	-	28
aluminum	16	-
plastics	55	8

Table 7: Material decomposition of the three sectors of the supply tube in [g] per half-shell. The term "plastics" refers to different kinds of polymers of similar density such as polyesther, polyvinylchloride and polyoxymethylene.

sector	A	B	C
aluminum	610	746	470
FR4	653	517	517
Airex®	80	69	30
steel	351	223	94
copper	51	283	150
plastics	610	1740	720
coolant	330	828	346

4.1 Central Barrel

A pixel barrel module is represented by several boxes of different thicknesses stacked on top of each other. Their dimensions are:

- base plates: $0.45\ \mathrm{cm} \times 6.6\ \mathrm{cm} \times 300\ \mu\mathrm{m}$, There are two baseplates per full module positioned at the module edges,
- silicon sensors: $1.9\ \mathrm{cm} \times 6.6\ \mathrm{cm}\ \times 285\ \mu\mathrm{m}$,
- High Density Interconnect (HDI): $1.9\ \mathrm{cm} \times 6.5\ \mathrm{cm} \times 44\ \mu\mathrm{m}$,
- Read-Out Chip (ROC): $2\ \mathrm{cm} \times 6.5\ \mathrm{cm} \times 180\ \mu\mathrm{m}$.

Four additional cuboidal volumes are defined for each module to describe localized components such as capacitors and TBM chips. These are visualized in Figure 7. The capacitors along the module edge are implemented as strips of $6.5\ \mathrm{cm}$ length and $0.5\ \mathrm{mm} \times 0.5\ \mathrm{mm}$ cross section.

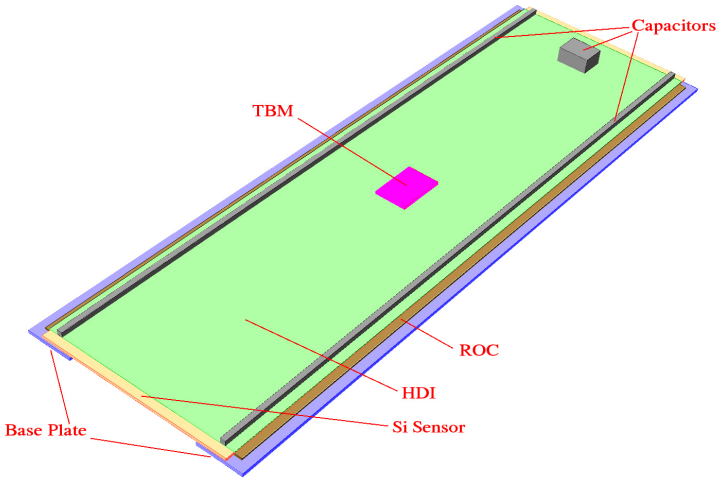

Figure 7: A full barrel pixel module in the Monte Carlo simulation.

The modules are replicated to form ladders and then layers, starting from the single module description contained in the XML.

The cooling pipes of the central barrel support structure have trapezoidal cross sections with various inclination angles (see Figure 2). The angles are computed automatically by the software given the number of ladders and the corresponding radius of the layer. The carbon fiber ladders holding the modules are represented as rectangles of $2.6\ \mathrm{cm}$ width and $250\ \mu\mathrm{m}$ thickness, running along the full length of the barrel ($53\ \mathrm{cm}$). There are 16 holes in the ladders, two under each module, of $2.2\ \mathrm{cm}$ length and $1.1\ \mathrm{cm}$ width to reduce the amount of material.

For the cables, we use four different types of volumes to account for the different lengths (23, 16, 9 and 3 cm), reaching modules at different longitudinal positions. Cable volumes are boxes with cross sections of $300\ \mu\mathrm{m} \times 0.67\ \mathrm{cm}$ running from the module (at a distance of $1.93\ \mathrm{cm}$ from the module edge) to the endflange. The remaining length of the cable is accounted for in the endflange description. The volumes of the cables are replicated in their proper positions to form the layers.

The half-ladders are described in a similar way and their volumes are located in the top and bottom edges of each half-shell.

4.2 Endflange

The logical volumes forming the endflange are implemented as circular disks and rings, except for the cooling, which only covers an azimuthal angle of $\Delta\phi = 140^\circ$ (Figure 8). They are located at a distance $z = \pm 28\ \mathrm{cm}$ from the detector center.

The parts labelled "inner flange" represent the arcs belonging to layers 1 and 2. Their material is composed of the glass fiber and carbon fiber frame, including the aluminum manifolds, and the contained coolant. The innermost part of the outer flange is implemented analogously (third ring in Figure 8). The second part of the outer flange extends further in radius (up to $18.6\ \mathrm{cm}$) and does not contain any cooling manifold.

The endring prints and cables are mounted onto the outer flange. The cables between the detector modules and the endring prints are labelled "radial cabling". The radial cabling extends up to a maximal radius of $17\ \mathrm{cm}$ as visible in Figure 4. This volume contains the remaining fraction of the central barrel signal cables.

There is an additional volume (not shown in Figure 8) implemented as a ring at $z = \pm 30.5\ \mathrm{cm}$ and $r = 18\ \mathrm{cm}$ which contains the signal and power cables connecting the endring prints with the supply tube. This ring also includes the innermost part of the supply tube which is labelled "Inner Flange" in Figure 6.

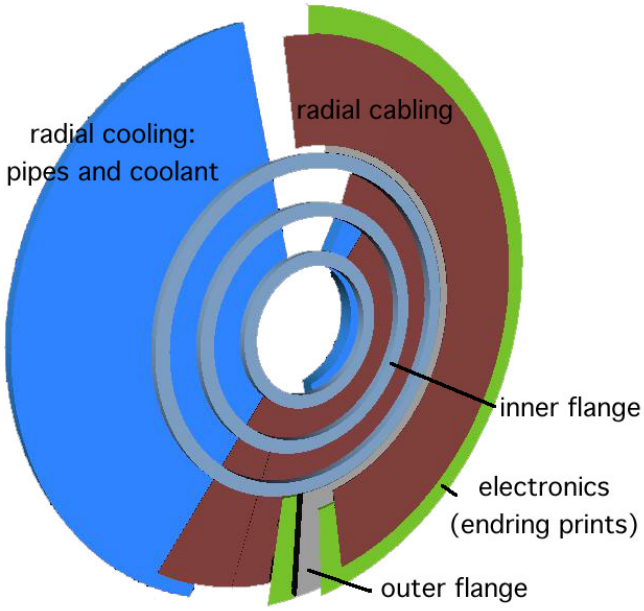

Figure 8: Cross section of the endflange in the Monte Carlo simulation. The various volumes are clipped for better visibility (except for the radial cooling).

4.3 Supply Tube

The representation of the supply tube is straightforward. Each of the three sectors described in Section 2.3 and Figure 6 is represented as a single volume with an average material content according to Table 7. There are three cylinders, one for each sector with inner radius of $r = 18\ \mathrm{cm}$ and wall thickness of $2.5\ \mathrm{cm}$. The lengths of Sectors A, B and C are 48.5, 120 and $49.3\ \mathrm{cm}$, respectively.

As discussed in the last paragraph of the previous section, the circular "Inner Flange" of the supply tube is implemented as a separate ring which also contains the steel connections for the cooling pipes and cabling.

5 Results and Summary

After the final assembly of the pixel barrel detector, the weight of one completed half-shell was measured (without coolant). Figure 9 shows one final half-detector on a balance. The cables and cooling tubes between supply tube and detector endflange were not included in this measurement. The result was $2598\ \mathrm{g} \pm 0.5\ \mathrm{g}$.

For comparison, the weight of this configuration in the Monte Carlo simulation is $2455\ \mathrm{g}$. The remaining disagreement is around 6% and is due to the unavoidable approximations as discussed in Section 3.

Figure 10 shows a $r - z$ profile of the detector as it is implemented in the Monte Carlo simulation. In Figures 10 to 12, the material is averaged over the azimuthal angle ϕ.

The integrated material as experienced by particles emerging from the interaction point and traveling on straight lines through the detector is shown in Figure 11.

Figures 12 and 13 show the integrated material budget in terms of radiation lengths for all components of the CMS tracker, including the pixel detector. The main pixel contribution to the material budget is in the region at $|\eta| > 1.2$ and is due to the material in the endflange and the inner part of the supply tubes. Therefore, future detector upgrades will concentrate on the reduction of the material in these components.

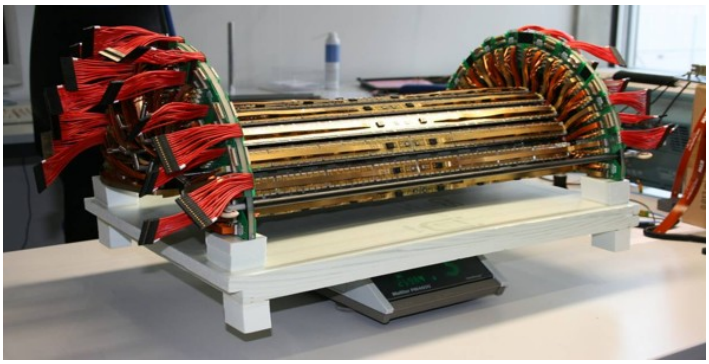

Figure 9: The completed PXB half-shell on a balance which shows the weight of $2598\ \mathrm{g}$. Not included are the coolant and the signal cables to the supply tube.

References

[1] The CMS Collaboration, "The CMS experiment at the CERN LHC", J. Inst. **3** (2008) S08004.

[2] The CMS Collaboration, "Tracker Technical Design Report", CERN/LHCC 98-6 (1998).

[3] The CMS Collaboration, "Addendum to the CMS Tracker TDR", CERN/LHCC 200-016 (2000).

[4] H. C. Kästli et al., "CMS barrel pixel detector overview", Nucl. Instrum. Meth. A **582** (2007) 724.

[5] S. König et al., "Building CMS pixel barrel detector modules", Nucl. Instrum. Meth. A **582** (2007) 776.

[6] Y. Allkofer et al., "Design and performance of the silicon sensors for the CMS barrel pixel detector", Nucl. Instrum. Meth. A **584** (2008) 25.

[7] H. C. Kästli et al., "Design and performance of the CMS pixel detector readout chip", Nucl. Instrum. Meth. A **565** (2006) 188.

[8] D. Kotlinski et al., "The control and readout systems of the CMS pixel barrel detector", Nucl. Instrum. Meth. A **565** (2006) 73.

[9] S. König et al., "Assembly of the CMS pixel barrel modules", Nucl. Instrum. Meth. A **565** (2006) 62.

[10] laser welding: CREATECH AG, Gaswerkstrasse 67, CH-4901 Langenthal, Switzerland: `http://www.createch.ch`

[11] ALCAN AIREX AG, CH-5643 Sins, Switzerland: `http://www.alcanairex.com`

[12] S. Agostinelli et al., "GEANT4 - A Simulation Toolkit", Nucl. Instrum. Meth. A **506** (2003) 250.

[13] J. Allison et al., "Geant4 developments and applications", IEEE Transactions on Nuclear Science **53** (2006) 270.

[14] M. Case et al., "Detector Description Domain Architecture and Data Model", CMS Note **2001-057** (2001).

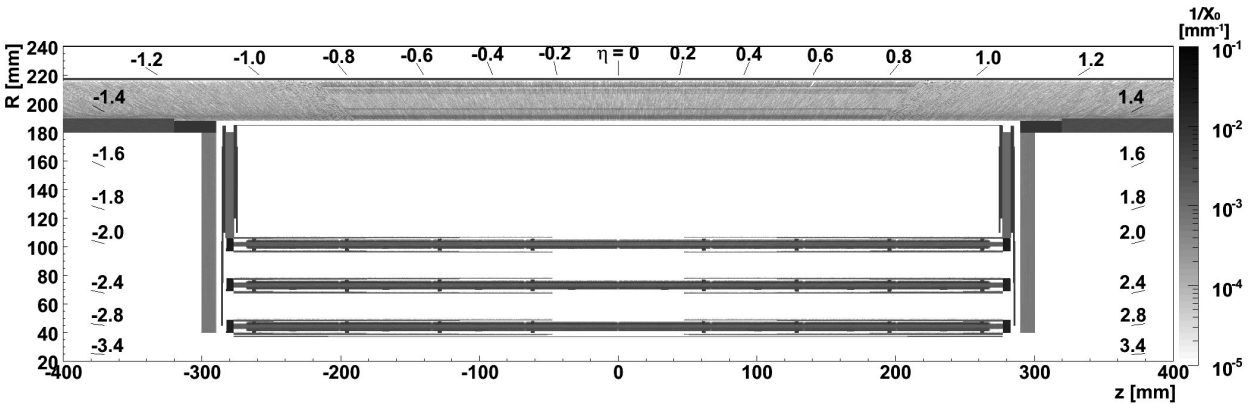

Figure 10: $r - z$ profile of the PXB detector (as implemented in the simulation). The grayscale indicates the inverse of the radiation length $1/X0(r, z, \phi)$ averaged over ϕ, at a given point in space. The pseudo-rapidity η is visualized near the upper, left and right edges of the diagram.

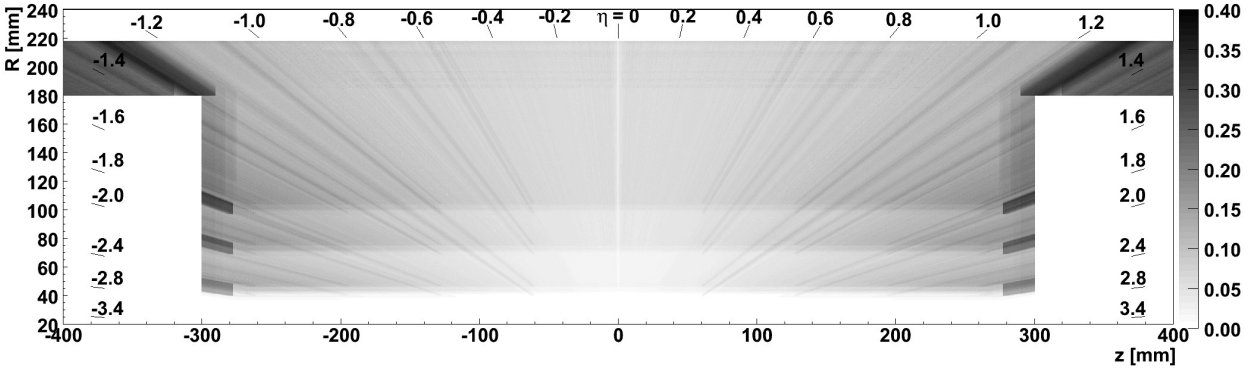

Figure 11: Integrated radiation length x/X_0 experienced by particles emerging from the interaction point as a function of pseudo-rapidity, averaged along ϕ. The grayscale indicates the number of radiation lengths traversed by a particle propagating on a straight line.

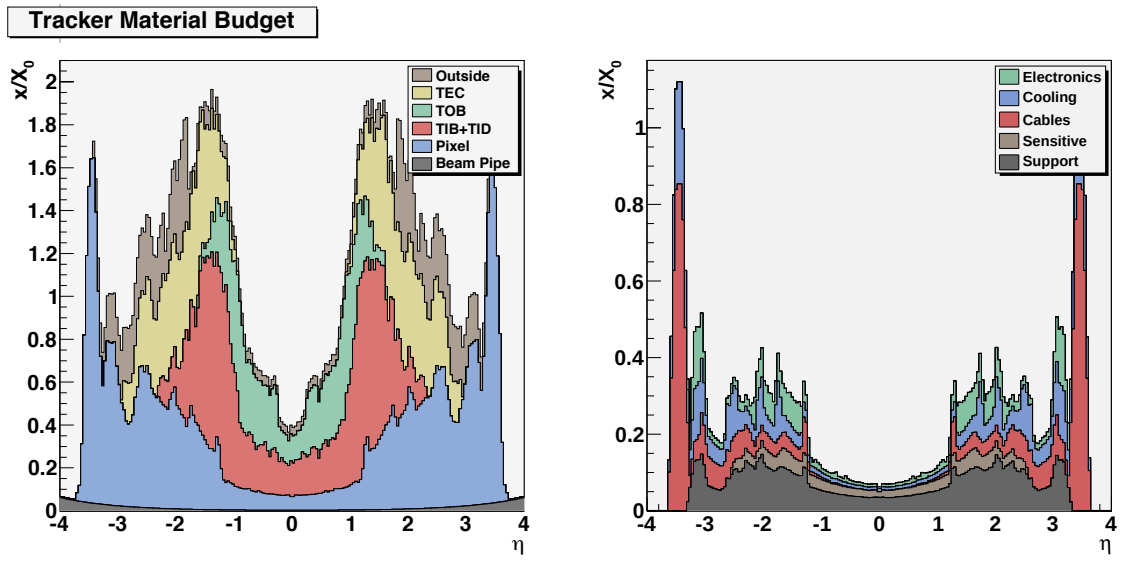

Figure 12: Left: total integrated material budget of the CMS tracker in terms of radiation lengths x/X_0 as a function of pseudo-rapidity, including the forward pixel detector. The contributions of the various subdetectors are stacked. Right: material budget for the pixel barrel detector only, showing the various categories of material.

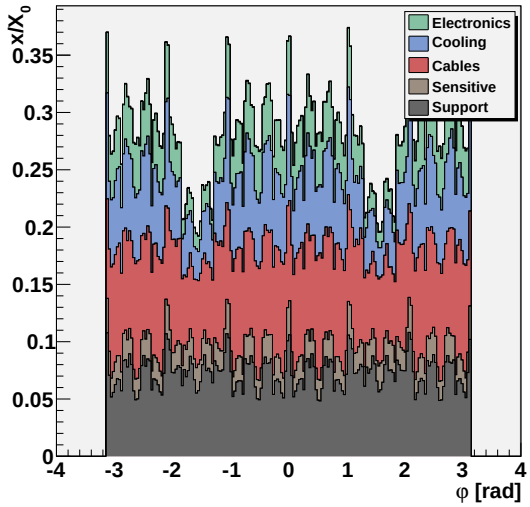

Figure 13: Total integrated material budget of the pixel barrel detector in terms of radiation lengths x/X_0 as a function of the azimuthal angle ϕ, averaged over the pseudo-rapidity η. The two gaps at $|\phi| = \pm 1.6$ are due to the asymmetry of the supply tubes.